

## **I-1. PROJECT RESEARCHES**

### **Project 4**

## Chemical and electronic properties of Actinide compounds and their applications

T. Yamamura, Y. Haga<sup>1</sup>, M. Abe<sup>2</sup>, M. Nakase<sup>3</sup>, K. Shirasaki<sup>4</sup>, S. Kambe<sup>1</sup>, N. Ishikawa<sup>5</sup>, T. Suzuki<sup>6</sup>, M. Nogami<sup>7</sup>, T. Kobayashi<sup>1</sup>

*KURNS Kyoto University, <sup>1</sup> Advanced Science Research Center, JAEA <sup>2</sup> Graduate School of Advanced Science and Engineering, Hiroshima University, <sup>3</sup> Institute of Integrated Research, Institute of Science Tokyo, <sup>4</sup> Institute for Radiation Sciences, Osaka University, <sup>5</sup> Department of Chemistry, Graduate School of Science, Osaka University, <sup>6</sup> Nagaoka University of Technology, <sup>7</sup> Graduate school of Electronic Eng., Kindai University*

**INTRODUCTION:** The 2024 fiscal year marks the second full cycle of the multi-institutional project aimed at elucidating the chemical and electronic properties of actinide 5f systems and translating them into practical applications in condensed-matter physics, coordination chemistry, separation science, and medical isotopes. The hot laboratories at the Institute for Integrated Radiation and Nuclear Science, Kyoto University, continue to provide the required infrastructure for handling gram-scale quantities of actinide materials. Building on the instrumentation and methodologies commissioned in 2023, the consortium expanded to nine research teams.

### RESULTS AND DISCUSSIONS:

**I. Metallic Intermetallic Physical Properties** 1. Actinide Intermetallic Compounds (Haga, R6P4-1): Single-crystal X-ray diffraction revealed that replacing Ge with Si in ThRh<sub>6</sub>Ge<sub>4</sub> destabilises the LiRh<sub>6</sub>P<sub>4</sub>-type structure. Weak super-lattice reflections emerge along the c\* axis, indicating the onset of lattice softening that precedes a possible charge-density-wave state. 2. Hidden-Order Physics in URu<sub>2</sub>Si<sub>2</sub> (Kambe, R6P4-5): Temperature-dependent <sup>101</sup>Ru NQR spectra under uniaxial stress  $\sigma[100] = 0.23$  GPa showed that the electric-field-gradient symmetry at the Ru site remains four-fold down to 1.5 K, supporting an order parameter that preserves the C<sub>4</sub> point group even in the hidden-order phase. 3. Physical Properties of Simulated Fuel Debris (Kobayashi, R6P4-9): Sample fabrication was delayed owing to beam-time scheduling at external hot cells. A contingency plan to synthesise three surrogate debris compositions (U,Zr,Ca)O<sub>2-x</sub> using spark-plasma sintering has been approved for early R7.

**II. Theoretical Chemistry** 4. Relativistic Multireference Electronic-Structure Theory (Abe, R6P4-2): The newly released X2C–RASPT2 program reproduces the vertical  $1\Sigma_u^+ \rightarrow 1\Sigma_g^+$  transition of UO<sub>2</sub><sup>2+</sup> within 0.08 eV of spin–orbit CASPT2 and EOM-CCSD benchmarks. The code enables active spaces up to (24e,24o) with DMRG optimisation.

**III. Coordination Chemistry** 5. Data-Driven Discovery of Phthalocyanine Extractants (Nakase, P4-3): The AACE workflow clustered 512 synthetically accessible Pc derivatives by Hansen solubility parameters and  $\pi$ -electron descriptors. Twenty-four candidates were prioritised for synthesis, halving experimental overhead compared with the brute-force search in R5. 6. Spectroscopy of U–Porphyrin/Phthalocyanine Complexes (Ishikawa, R6P4-6): Variable-temperature MCD of U(TPP)Cl<sub>2</sub> exhibited a sign inversion of the Q-band at 92 K, suggesting thermal population of spin-orbit split 5f<sup>2</sup> manifolds that couple to the porphyrin  $\pi$  system.

**IV. Separation Chemistry** 7. U(VI) Adsorption by Silica-Supported DMAA–TPMA Resin (Nogami, R6P4-8): A two-step grafting protocol afforded a hybrid resin whose distribution coefficient  $K_d(\text{U})$  exceeds that for Ce<sup>3+</sup> by an order of magnitude up to 6 M HNO<sub>3</sub>. Batch adsorption isotherms followed a Langmuir model with  $Q_{\text{max}} = 52$  mg-U g<sup>-1</sup>.

**V. Medical-Isotope Separation and Purification** 8. Extraction Chemistry of <sup>228</sup>Ac with D2EHPA (Shirasaki, R6P4-4): Log–log plots of D<sub>Ac</sub> versus [(D2EHPA)<sub>2</sub>] yielded a slope of  $3.0 \pm 0.1$ , consistent with a tri-dimeric extraction complex. At pH<sub>ini</sub> 6.0 the distribution ratio exceeded 10<sup>3</sup>, paving the way for one-cycle purification schemes. 9. Separation of <sup>228</sup>Ra for <sup>225</sup>Ac/<sup>229</sup>Th Production (Suzuki, R6P4-7): Combining PVPP chromatography with MgCO<sub>3</sub> co-precipitation achieved 92 % retention of <sup>228</sup>Ra on MgO, while reducing Th carry-over below 0.05 %. The eluate meets radio-chemical purity targets for generator fabrication.

## Crystal Structure and Characterization of Actinide Intermetallic Compounds

Y. Haga

Advanced Science Research Center, Japan Atomic Energy Agency

**INTRODUCTION:** Actinide elements and their compounds are known to show unique physical properties. Actinides are often compared with lanthanides where both series of elements are characterized by f-shell electrons. As demonstrated by the complicated crystal structures of some of the actinide metals, unlike those of rare earth metals, the difference of electronic structure between these series might be involved in the crystal structure. Here, we report a comparison of isostructural lanthanide and actinide compounds,  $ARh_6X_4$  ( $A$  = actinide or lanthanide,  $X$  = Si, Ge) crystallizing in the hexagonal structure, an analog of the heavy fermion ferromagnet  $CeRh_6Ge_4$ . [1]

**EXPERIMENTS:** The samples of ternary Th-Rh-Ge and Th-Rh-Si systems were synthesized by arc-melting with the starting composition 1:6:4. The crystal structures were measured by single-crystal X-ray diffraction on a single crystal extracted from the arc-melted ingot.

**RESULTS:** We confirmed that  $ThRh_6Ge_4$  crystallizes in the hexagonal  $LiCo_6P_4$ -type structure. The cerium analog  $CeRh_6Ge_4$  is reported to have the same structure. Because the formal valence electron count for both compounds are the same, electronic structure should also look alike. In fact we have already investigated electronic structure of  $ThRh_6Ge_4$  [2] to discuss the correlated electronic behavior in  $CeRh_6Ge_4$ . However, when Ge is replaced by Si, this structure became unstable. Figure 1 shows the X-ray diffraction data mapped on (0 0 1) plane for  $ThRh_6Ge_4$  and “ $ThRh_6Si_4$ ”. In  $ThRh_6Ge_4$ , the reflections are indexed as hexagonal cell. In the “ $ThRh_6Si_4$ ”, however, the diffraction data is completely different. Although strong reflections marked by large circles approximately maintain the similar hexagonal symmetry, there are weak super reflections. This result directly demonstrates that the structural instability occurs when Si is substituted, most likely caused by the Fermi surface instability. The detailed structural analyses are in progress.

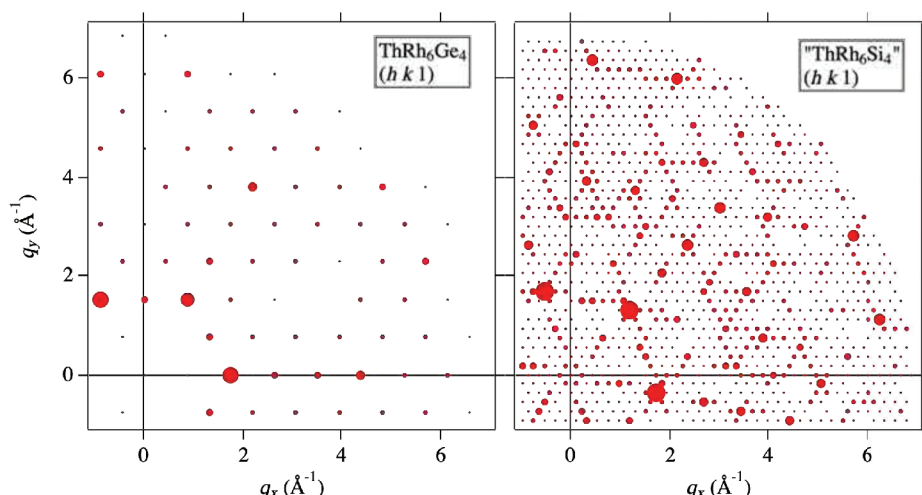


Fig. 1. X-ray diffraction data for  $ThRh_6Ge_4$  and “ $ThRh_6Si_4$ ”.

### REFERENCES:

- [1] H. Kotegawa *et al.*, J. Phys. Soc. Jpn., **88** (2019) 093702.
- [2] Y. Haga *et al.*, International Conference on Strongly Correlated Electron Systems 2023.

## Development of relativistic multireference electron correlation methods for actinide compounds

M. Abe,<sup>1</sup> Y. Masuda,<sup>1</sup> S. Toda,<sup>1</sup> T. Yamamura<sup>2</sup>

<sup>1</sup> Department of Chemistry, Hiroshima University

<sup>2</sup> Institute for Integrated Radiation and Nuclear Science, Kyoto University

**INTRODUCTION:** Understanding the properties of actinide compounds is crucial for both engineering and academic research. Theoretical calculations, alongside experimental approaches, play a vital role in elucidating their characteristics and facilitating safe verification studies. However, accurately handling relativistic and electron correlation effects is essential for theoretical investigations of actinide compounds. As the atomic number  $Z$  increases, the relativistic effect becomes significant, challenging the accuracy of conventional scalar relativistic treatments or perturbative corrections of spin-orbit interactions. Rigorous relativistic effects demand the application of four-component Dirac or exact two-component (X2C) relativistic Hamiltonians. Moreover, because all s, p, d, and f orbitals serve as valence orbitals for actinide atoms, static electron correlation cannot be neglected, limiting the efficacy of conventional single reference methods like density functional theories. Multi-reference electron correlation theory becomes necessary but poses computational challenges due to its complexity. Our group has developed new quantum chemistry programs based on the X2C relativistic Hamiltonian to accurately calculate electronic states and properties of actinide compounds. Specifically, we have created a program for the CASPT2/RASPT2 method, employing multiconfigurational wave functions (CASCI/RASCI) as the 0th-order state of perturbation. CASPT2/RASPT2 is a well-established perturbation theory in the non-relativistic framework [1].

**METHODS:** The Hartree-Fock and molecular orbital integral transformation with the X2C relativistic Hamiltonian can be executed using the free software DIRAC [2,3]. Consequently, we have developed a CASPT2/RASPT2 program that utilizes molecular orbital information computed by the DIRAC software.

**RESULTS:** This year, we released our newly developed program as an open-source project on GitHub [4] and reported benchmark calculations of the vertical excitation energies of the  $\text{UO}_2^{2+}$  ion [5]. Because these excitations require a large active space, we applied the RASPT2 method. Figure 1 compares our results with those from previous studies. Our highest-accuracy protocol—RASPT2(3h,3e) incorporating Improved Virtual Orbitals (IVO)—yields excitation energies very close to EOM-CCSD and SO-CASPT2 benchmarks, whereas four-component TDDFT and IHFSCCSD show larger deviations. These observations indicate that, for the excited states studied here, the choice of electron-correlation treatment has a greater impact on accuracy than the relativistic Hamiltonian.

### REFERENCES:

- [1] K. Anderson *et al.*, J. Phys. Chem., **94** (1990) 5483–5488.
- [2] H. J. Aa. Jensen *et al.*, DIRAC, a relativistic ab initio electronic structure program, Release DIRAC22 (2022).
- [3] T. Saue *et al.*, J. Chem. Phys. **152** (2020) 204104.
- [4] The software is downloadable from [https://github.com/RQC-HU/dirac\\_caspt2](https://github.com/RQC-HU/dirac_caspt2)
- [5] Y. Masuda *et al.*, J. Chem. Theory Comput., **21** (2025) 1249–1258.

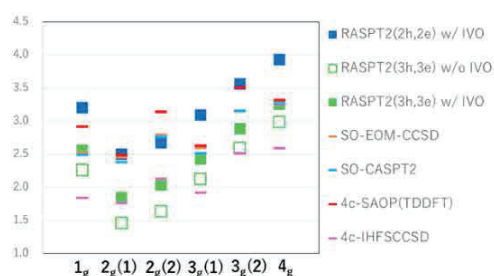


Fig. 1. Vertical excitation energies of  $\text{UO}_2^{2+}$  molecule

## Synthesis of novel phthalocyanine derivatives and the effect of substituent on the recognition of light actinide and chemical property-4

M. Nakase<sup>1</sup>, F. Ikhwani<sup>1</sup>, T. Yamamura<sup>2</sup>

<sup>1</sup>*Institute of Innovative Research, Tokyo Institute of Technology*

<sup>2</sup>*Institute for Integrated Radiation and Nuclear Science, Kyoto University*

**INTRODUCTION:** Understanding actinide chemistry is crucial in the reprocessing of spent nuclear fuels, Fukushima waste treatment, and medical uses of actinium. My focus is on the Th fuel cycle, which avoids producing heavy actinides like Am and Cm, instead dealing with light actinides such as Th, Pa, and U. This cycle requires separating U from Th and other fission products in spent Th fuels. Recently, we investigated the use of phthalocyanine (Pc) derivatives as extractants for U/Th separation. This year, experiments were not conducted for several reasons; however, the chemoinformatic approach progressed.

**INFORMATIC APPROACH:** The scheme for exploring the extractant structure is as follows: First, structural data, physicochemical properties (calculated by regression using Hansen Solubility Parameter (HSP) values), and some calculated energy parameters are compiled. The structural fingerprint is created based on the Simplified Molecular Input Line Entry System (SMILES). Clustering methods are used to predict solubility, and the extraction performance is also predicted. All the steps of the approach are compiled in the computational program, Acceleration of Actinide Chemistry Experiment (AACE), which can deploy transfer learning (TL) and human-in-the-loop machine learning (HITL-ML) [1]. The code is written in Python, and modules are combined using Streamlit, which enables the creation of simple user interfaces and facilitates machine learning with reduced coding effort.

**RESULTS:** The functionalities and the operation check of the AACE program were completed, and an initial ML attempt was done by using the extracted data obtained for the other research project. To implement machine learning to find suitable Pc-derivatives for reprocessing Th-based fuels, we need more data.

**CONCLUSION:** The Pc-derivatives suitable for reprocessing in the Th-U fuel cycle were attempted by an informatics approach. The biggest hurdle was the synthesis part, which was difficult to accelerate in the current situation of my laboratory. Therefore, from the next fiscal year, we will focus our research more on informatics, utilizing data from previously published papers and databases, and, where possible, data collected at Kyoto University.

### REFERENCES:

[1] M. Nakase *et al.*, EPJ Web of Conf., **317** (2025) 01007.

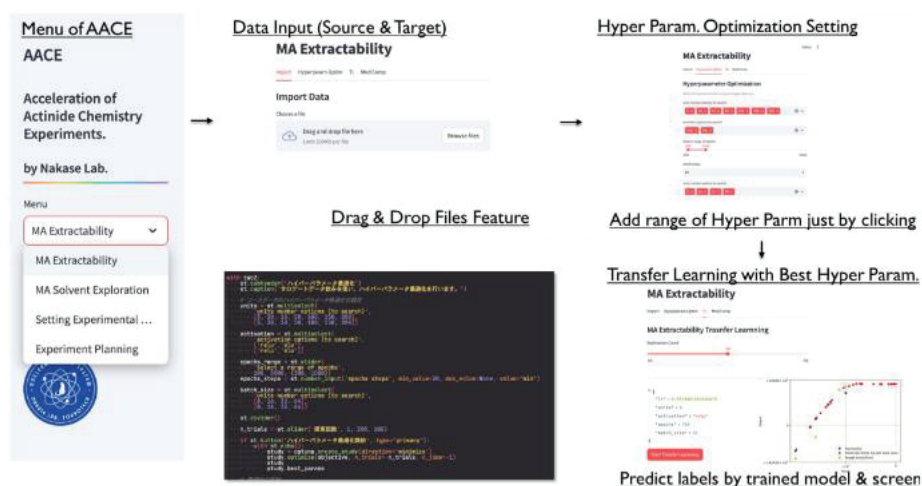


Fig. 1. AACE program developed in 2025 at Nakase-lab [1]



## Evaluation of extraction behavior of $^{228}\text{Ac}$ by D2EHPA under pH range.

K. Shirasaki and T. Miyawaki<sup>1</sup>

*Institute for Radiation Science, The University of Osaka*

*<sup>1</sup> Institute for Materials Research, Tohoku University*

**INTRODUCTION:** Actinium is the earliest element in the actinide series, which has 29 isotopes excluding metastable states, and is considered similar to lanthanum in chemical properties. In terms of oxidation state, actinium has only trivalent state like the elements after americium in the actinide series. Most isotopes of actinium are produced by nuclear reactions and have short half-lives of a few seconds to a few minutes.  $^{225}\text{Ac}$ , one radioisotope of actinium, is used in targeted alpha therapy and has been reported to be highly effective to the cancer therapy, especially for prostate cancer [1].  $^{225}\text{Ac}$  is very therapeutic because it undergoes four alpha decays before becoming stable  $^{209}\text{Bi}$  and does not pass through a noble gas. However, the resources of actinium isotopes, not only  $^{225}\text{Ac}$  but also  $^{227}\text{Ac}$  are quite rare and expensive.  $^{228}\text{Ac}$ , one of the thorium series, reaches radiolytic equilibrium with the parent nuclide  $^{228}\text{Ra}$  in about 30 hours. Therefore, once separated, the same amount of  $^{228}\text{Ac}$  can be collected again [2].  $^{228}\text{Ac}$  emits photons over a wide energy range and its emission rate is very high among isotopes. With these properties,  $^{228}\text{Ac}$  is expected to facilitate basic research on actinium, such as chelate chemistry, which is also required for labeling.

In this study, the extraction behavior of  $^{228}\text{Ac}$  and La by D2EHPA in the pH range is evaluated using shaking time, extractant concentration dependence, and pH as indicators for study basic coordination chemistry of actinium.

**EXPERIMENTS:** Here, the buffer ADA is used as the aqueous phase, and n-dodecane (nDD), one of hydrocarbonate solvents with properties such as nonflammability, chemical stability and low viscosity, were used as the organic phase. Initially,  $^{228}\text{Ac}$  was dissolved in the aqueous phase. Under the pH condition,  $^{228}\text{Ac}$  in the aqueous phase was extracted into the organic phase by chelation between actinium and the D2EHPA compound. Here, the distribution ratio was used as an index to evaluate how much  $^{228}\text{Ac}$  in the aqueous phase was extracted into the organic phase.

**RESULTS:** The distribution ratio of  $^{228}\text{Ac}$  ( $D_{\text{Ac}}$ ) increased with increasing extractant concentration (Fig. 1). The slope obtained from the fit in the range  $-0.2 < \Delta\text{pH} < 0$  was  $3.38 \pm 0.2$  at  $\text{pH}_{\text{ini}} 6.0$ . Based on the extraction data, we can compare the extractant distribution ratios of other compounds to determine the effect of side chains, and to devise and demonstrate extractants and buffers that are compatible with Ac. For more investigations, such as the extraction behavior of actinium and extraction data for heavy actinide elements, which have the same trivalent stable state as Ac and Am, are needed to clearly demonstrate the similarity between actinide and lanthanide series elements.

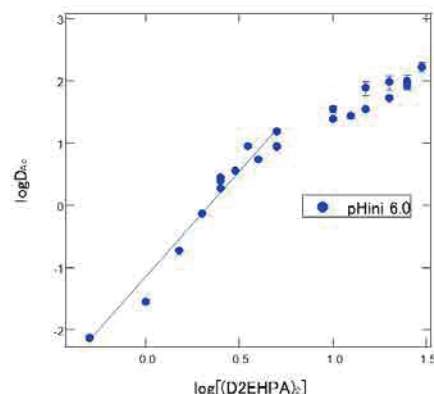


Fig. 1. Dependence of  $\log D_{\text{Ac}}$  vs.  $\log[(\text{D2EHPA})_0]$

## REFERENCES:

- [1] C. Kratochwil *et al.*, J Nucl Med. **57**(12) (2016) 1941-1944.
- [2] K.E. Aldrich *et al.*, In-organic Chemistry, **59**(5) (2020) 3200-3206.

## Study of Heavy Fermion Superconductor URu<sub>2</sub>Si<sub>2</sub> <sup>101</sup>Ru-NQR study II

S. Kambe, Y. Haga, H. Sakai, T. Ishitobi, Y. Tokunaga, H. Matsumura<sup>1</sup>, S. Kitagawa<sup>1</sup>, K. Ishida<sup>1</sup> and T. Yamamura<sup>2</sup>

*Advanced Science Research Center, Japan Atomic Energy Agency*

<sup>1</sup>*Department of Physics, Kyoto University*

<sup>2</sup>*Institute for Integrated Radiation and Nuclear Science, Kyoto University*

**INTRODUCTION:** Understanding of "Hidden ordering" in URu<sub>2</sub>Si<sub>2</sub> is fairly progressed recently [1], whereas the definitive answer is still missing. This issue is very exciting since the hidden ordering is supposed to be new spontaneous symmetry breaking. Considering the recent experimental results, a few possible space groups of hidden order symmetry have been selected previously [2,3]. If the hidden order symmetry is once determined, the corresponding multipolar order parameter is spontaneously determined.

**EXPERIMENTS:** In this study, the local symmetry of Ru site is determined in the hidden order state without uni-axial stress and with uni-axial stress along the [100] and [110] directions [4], by means of precise Ru-NQR measurements. These measurements again support the 4-fold symmetry at Ru site in the hidden order state without uni-axial stress. Furthermore, certain cases can be excluded from the previously proposed possible ones. In this year, the Ru-NQR measurements under uni-axial stress [100] direction are performed.

\*\*\*\*\*

**RESULTS:** Fig. 1 shows the T-dependence of <sup>101</sup>Ru NQR frequency at zero field under uni-axial stress  $\sigma$  along [100] direction of 0.23 GPa. As <sup>101</sup>Ru is  $I=5/2$  nuclei, there are two NQR peaks are observed i.e.  $\nu_{1Q}$  ( $I = \pm 3/2 \leftrightarrow I = \pm 1/2$ ) and  $\nu_{2Q}$  ( $I = 5/2 \leftrightarrow I = \pm 3/2$ ). In the present case, the  $\nu_{1Q}$  results are presented. Compared to the  $\sigma=0$  case, T-dependence is small in the case under [100] stress. This may be natural since  $\nu_{1Q}$  is related to the thermal expansion constant which is small in the c-plane due to  $\sigma[100]$ .

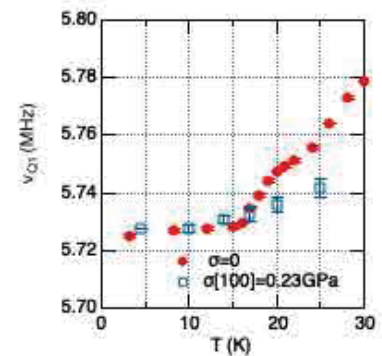


**Fig. 1.** T-dependence of <sup>101</sup>Ru NQR frequency at zero field under uni-axial stress  $\sigma[100]=0.23$  GPa.

## REFERENCES:

- [1] J. Mydosh *et al.*, J. Phys.:Condens. Matter, **32** (2020) 143002.
- [2] S. Kambe *et al.*, Phys. Rev. B, **97** (2018) 235142.
- [3] S. Kambe *et al.*, JPS Conf. Proc., **30** (2020) 011035.
- [4] See experimental methods: K. Karube *et al.*, J. Phys. Soc. Jpn., **83** (2014) 084706.

## Exploration of new interactions between actinide 5f electron systems and photo-excited organic $\pi$ -electron systems

N. Ishikawa, Ryosuke Amakatsu

Department of Chemistry, Graduate School of Science, Osaka University

**INTRODUCTION:** Metal complexes of actinide as well as those of lanthanide have high magnetic anisotropy due to the orbital angular momentum component in the total angular momentum of the f-electronic systems. In contrast to 4f electrons, 5f electrons are characterized by a large covalency involved in chemical bonding.

Another type of electronic angular momentum is known to be generated on a cyclic  $\pi$ -conjugated system of macrocyclic ligands, such as phthalocyanines (Pc) or porphyrins, by photo-excitation into degenerate  $\pi$ - $\pi^*$  excited states.

Previously, our group revealed the existence of a magnetic interaction between these two angular momenta (J-L interaction) in rare-earth Pc complexes by temperature- and magnetic-field-dependent magnetic circular dichroism (HT-VH-MCD) spectroscopy [1][2]. This interaction has been observed in sandwich-type bilayer complexes  $\text{Pc}_2\text{Ln}$  ( $\text{Ln}=\text{Tb}$ ,  $\text{Dy}$ ) and monolayer complexes  $\text{PcLn}(\text{cyclen})$ . Similar interaction was confirmed in the sandwich bilayer complex  $\text{Pc}_2\text{Ln}$  and the monolayer complex  $\text{PcLn}(\text{cyclen})$ . [3][4]

So far, we have conducted measurements of VT-VH-MCD in the visible energy region for the monolayer Pc complex of U(IV),  $\text{PcU}(\text{acac})_2$  ( $\text{acac}=\text{acetylacetonate}$ ), as well as the bilayer complex  $\text{Pc}_2\text{U}$  to investigate magnetic interaction between the  $(5f)^2$  system and the ligand  $\pi$ -conjugate system in a photo excited state.

This year, we conducted preliminary experiments for the synthesis of a new type of Pc-uranium complex having a different ligand, namely,  $\text{U}(\text{TPP})(\text{acac})_2$  ( $\text{TPP}=\text{tetraphenylporphyrinate}$ ).

**EXPERIMENTS:** The precursor  $\text{U}(\text{TPP})\text{Cl}_2$  was synthesized through the reaction of the metal-free  $\text{TPPH}_2$  and  $\text{UCl}_4$ . The obtained  $\text{U}(\text{TPP})\text{Cl}_2$  and  $\text{Na}(\text{acac})$  were placed in a flask in a glove box and THF was added. The mixture was then heated outside the glove box in a sealed condition using an oil bath. At the present stage, the target compound  $\text{U}(\text{TPP})(\text{acac})_2$  has not been identified. We have therefore conducted the VT-VH-MCD measurement of the precursor  $\text{U}(\text{TPP})\text{Cl}_2$  in a PMMA film.

**RESULTS:** Typical Soret band and Q band of metal porphyrins were observed in the visible region. Both bands exhibited temperature-dependent changes, but with completely opposite tendencies. The Soret band displayed a negative A-term pattern, with the MCD intensity increased as the temperature decreased. In contrast, the Q band exhibited a positive A-term pattern at 100 K, which gradually changed to a negative A-term pattern as the temperature decreased.

### REFERENCES:

- [1] K. Kizaki *et al.*, Chem. Commun., **53** (2017) 6168-6171.
- [2] T. Fukuda *et al.*, Chemistry A European Journal, **23(64)** (2017) 16357-16363.
- [3] K. Kizaki *et al.*, Inorg. Chem., **60(3)** (2021) 2037-2044.
- [4] K. Kizaki *et al.*, Inorg. Chem. Front., **10** (2023) 915-925.



## Fundamental Study on Extraction/Separation of Actinides and Their Decay Products for Medical Nuclide Production

T. Suzuki<sup>1</sup>, F. Yin<sup>1</sup>, S. Fukutani<sup>2</sup>, M. Harigai<sup>2</sup>, and T. Yamamura<sup>2</sup>

<sup>1</sup>Department of Nuclear System Safety Engineering, Nagaoka University of Technology

<sup>2</sup>Institute for Integrated Radiation and Nuclear Science, Kyoto University

**INTRODUCTION:** Many amounts of decay products are generated from uranium and/or thorium chemicals which are stored in long term. If these decay products are extracted and/or transmuted, we can obtain the several kinds of nuclides and can apply them to many fields such as medicine. While, concern of nuclear therapy using  $\alpha$ -nuclides recently increases. Especially,  $^{225}\text{Ac}$  is one of the most concerning  $\alpha$ -nuclides. However, since  $^{225}\text{Ac}$  don't exist in nature, it must be generated artificially. We have proposed  $^{229}\text{Th}/^{225}\text{Ac}$  generator,  $^{229}\text{Th}$  is generated by  $^{228}\text{Ra}(\text{n},\gamma)$  reaction. Our plain of obtaining  $^{228}\text{Ra}$  is recovery of decay products from Th. We have plan to use the residue of rare earth ore and/or long storage  $\text{ThO}_2$ . For obtaining this type generator, development of the dissolution method of thorium compounds, extraction of  $^{228}\text{Ra}$  from thorium and other decay products, manufacturing of stable target, irradiation of neutron, and separation of  $^{229}\text{Th}$ , etc. are required. In this fiscal year, we investigated the separation of  $^{228}\text{Ra}$  from  $^{229}\text{Th}$  by polyvinylpolypyrrolidone (PVPP), the coprecipitation of  $^{228}\text{Ra}$  separated by PVPP with  $\text{MgCO}_3$ , and the chemical conversion of  $\text{MgCO}_3$  with Ra to  $\text{MgO}$  with Ra.

**EXPERIMENTS:** Th solutions dissolved by thermochemical conversion method using  $\text{CBr}_4$  were used. The separation experiment of Ra from Th was carried out using a column packed with 1.12 g of PVPP. This column height was approximately 5 cm. The solution with the isolated Ra was neutralized by  $\text{NaCO}_3$ . Then, 8mL of 1M  $\text{NaCO}_3$  solution and 2mL of 1M  $\text{MgCl}_2$  solution were added in the Ra solution. The obtained  $\text{MgCO}_3$  precipitation was filtered.  $\text{MgCO}_3$  was converted to  $\text{MgO}$  by heating at  $400^\circ\text{C}$  for 0.5h. The transfer rate of Ra from solution to precipitation and the retention rate of Ra from carbonate to oxide were evaluated. The radioactivity of  $^{228}\text{Ra}$  was determined by  $\gamma$ -ray measurement of radio equilibrium  $^{228}\text{Ac}$ , which is daughter of  $^{228}\text{Ra}$ .

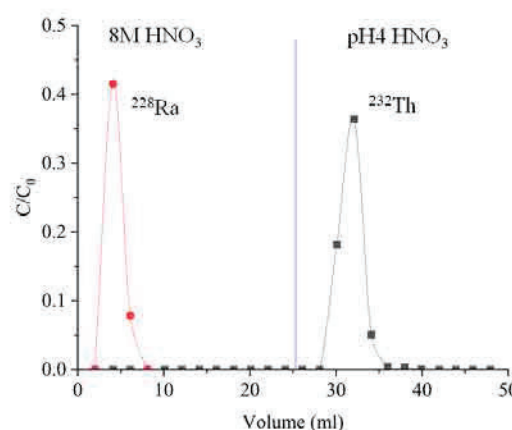


Fig. 1. Separation result of Ra from Th by PVPP.

**RESULTS:** Separation result of Ra from Th by PVPP was shown in Fig. 1. We can see the complete separation of Ra from Th. The transfer rate of Ra from solution to precipitation and the retention rate of Ra from  $\text{MgCO}_3$  to  $\text{MgO}$  are shown in Table.1 From this table, we confirmed that almost all Ra is transfer from solution to precipitation by  $\text{MgCO}_3$  precipitation method, and almost all Ra is remained in  $\text{MgO}$  after conversion from  $\text{MgCO}_3$  to  $\text{MgO}$ .

Table 1. Transfer rate of Ra from solution to precipitation, and retention rate of Ra in  $\text{MgO}$

Radioactivity of Ra in solution (Bq)	Radioactivity of Ra in $\text{MgCO}_3$ (Bq)	%transfer of Ra from solution to $\text{MgCO}_3$	Radioactivity f Ra in $\text{MgO}$ (Bq)	%retention of Ra in $\text{MgO}$
$5.56 \pm 0.77$	$5.28 \pm 0.57$	$95.0 \pm 16.7$	$4.87 \pm 0.58$	$92.2 \pm 14.8$

## Synthesis and Adsorptivity of Novel Bifunctional Monoamide- Diamide Resin for Selective Separation of Actinyl Ions

M. Nogami, K. Uchida, S. Matsumoto <sup>1</sup>, C. Abe <sup>2</sup>, M. Toyama <sup>3</sup>, and T. Yamamura <sup>3</sup>

Faculty of Science and Engineering, Kindai University

<sup>1</sup>Graduate School of Science and Engineering, Kindai University

<sup>2</sup>Institute for Materials Research, Tohoku University

<sup>3</sup>Institute for Integrated Radiation and Nuclear Science, Kyoto University

**INTRODUCTION:** Development of highly selective compounds for hexavalent actinide species (actinyl ions, An(VI), AnO<sub>2</sub><sup>2+</sup>) has been important. We have been focusing on monoamide compounds which coordinate with An(IV) and (VI) species in nitric acid media as promising candidates. However, as reported last year[1], forming six-coordinated structures where one AnO<sub>2</sub><sup>2+</sup> ion is surrounded by two carbonyl oxygen atoms of two monoamide molecules might be difficult spatially in case of resins. In order to increase the possibility of these coordinations, we suggested the combined use of monoamide and diamide compounds as bifunctional groups. Diamide compounds are famous for separating not only An(IV) and (VI) species but also An(III) and lanthanide(III) (Ln(III)) ones. In this study, a preliminary synthesis and adsorptivity of a novel bifunctional monoamide-diamide resin was investigated.

**EXPERIMENTS:** *N,N*-dimethylacrylamide (DMAA) and *N,N,N',N'*-tetrapentylmalonamide (TPMA) were used as monoamide and diamide, respectively. The synthetic scheme of the resin has two steps as shown in Fig. 1. DMAA, chloromethylstyrene (CMS), and divinylbenzene (DVB) were firstly copolymerized (8 % crosslinkage) at the mixed ratio of DMAA/CMS = 1 (w/w) with pore producing solvents and a porous silica support similarly to the earlier literatures[2,3]. Chlorine atoms of poly-CMS were then substituted by TPMA by following the earlier literature[4] and the final resin (Silica DMAA-TPMA) was obtained. Adsorptivity of the resin was examined by a batch method using U(VI) and Ce(III) up to 6 mol/dm<sup>3</sup> (= M) HNO<sub>3</sub> at room temperature.

**RESULTS:** The resin showed adsorptivity basically with increasing concentration of HNO<sub>3</sub> for U(VI) and in HNO<sub>3</sub> higher than 3 M for Ce(III), Respectively. The *K<sub>d</sub>* values for U(VI) were more than 10 times higher than those for Ce(III). In addition, those for U(VI) of Silica DMAA-TPMA was found to be higher than those of Silica DMAA resins[2] although the direct comparison for experimental conditions would be difficult. This suggests that, as expected, bifunctional monoamide-diamide resins may improve adsorptivity for An(VI) by suppressing the adsorption for Ln(III). It was also revealed that the resin has some points to be improved, e.g., increase in adhesion ratio of the polymers to the silica support.

### REFERENCES:

- [1] M. Nogami *et al.*, KURNS Progress Report 2023 (2024) PR5-8.
- [2] M. Nogami *et al.*, J. Radioanal. Nucl. Chem., **273** (2007) 37-41.
- [3] M. Nogami *et al.*, Prog. Nucl. Energy, **50** (2008) 462-465.
- [4] M. Nogami *et al.*, J. Solid State Chem., **171** (2003) 353-357.

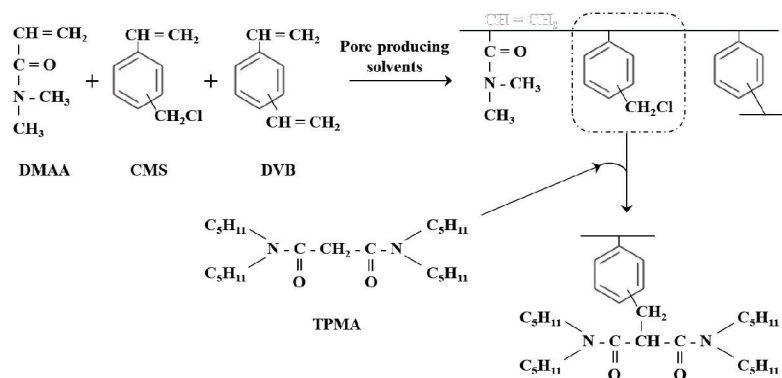


Fig. 1. Synthetic scheme of Silica DMAA-TPMA.